Photostriction of Sol–Gel Processed PLZT Ceramics

PATCHARIN POOSANAAS, A. DOGAN, A.V. PRASADARAO, S. KOMARNENI & K. UCHINO
International Center for Actuators and Transducers, Materials Research Laboratory, The Pennsylvania State University, University Park, PA 16802, USA

Abstract. Lanthanum-modified lead zirconate titanate (PLZT) ceramic materials have gained considerable attention due to their photostriction, which is the superposition of photovoltaic and piezoelectric effects. However, the photovoltaic effect and the induced strain response are also influenced by the fabrication and processing conditions. The PLZT ceramics produced by conventional oxide mixing process exhibit moderate photostrictive properties due to the inhomogeneous distribution of impurities. In this study, ceramics of PLZT (3/52/48) doped with WO_3 and Nb_2O_5 were prepared by sol–gel technique using lead(II) acetate trihydrate, lanthanum(III) acetylacetonate hydrate, Zr, Ti, Nb, and W alkoxides. It was found that WO_3 and Nb_2O_5 were effective in suppressing the grain growth of PLZT, which lead to the enhancement of photovoltaic and photostrictive properties. Photovoltaic and photostrictive responses showed a maximum for samples with 0.5 at% WO_3 doped sol–gel PLZT. It has been shown that the sol–gel derived PLZT ceramics with proper density possess the possibility of enhancing the photostriction over ceramics produced by conventional oxide mixing process.

Keywords: photostriction, photovoltaic effect, sol–gel, PLZT, doping effect, tungsten, niobium

Introduction

Lanthanum-modified lead zirconate titanate (PLZT) ceramics are known to exhibit a range of interesting electro-optical properties. The advantages of PLZT ceramics are their high optical transparency, desirable electrooptic properties, and fast response (Xu, 1991). There have been many successful demonstrations of the applications of PLZT. Recently, the application of PLZT in photostrictive actuators has drawn considerable attention (Uchino and Aizawa, 1985; Uchino et al., 1985; Sada et al., 1987; Chu et al., 1994; Chu and Uchino, 1995).

Photostrictive effect is the superposition of the photovoltaic and piezoelectric effects. This effect is of interest in the development of wireless remote control photodriven actuators. Another promising application will be in the new generation photoacoustic devices. Photovoltaic effect and the strain response have been shown to vary greatly for the different preparation processes, even in materials with the same composi-

tion (Sada et al., 1987). In a ceramic material for electro-optic application, a combination of good ferroelectricity and high transparency is required. This requirement can be met by a ceramic material with high density, low porosity, and a homogeneous composition. However, the conventional oxide mixing process provides inhomogeneous distribution of impurities, resulting in moderate photostriction properties. The sol–gel process, involving chemical precipitation (solution reaction) for preparation of powder materials, has gained attention in comparison to the conventional techniques due to its inherent advantages in producing high density homogeneous powder with a greater control on stoichiometry (Chiou and Kno, 1990; Rahaman, 1995). In addition, the obtained powders are finely divided and greatly enhanced in reactivity, sinterability and transparency over powders prepared by the conventional processing.

In this study, ceramics of PLZT (3/52/48) doped with WO_3 and Nb_2O_5 were prepared by both the

conventional oxide mixing process and the sol–gel technique using lead(II) acetate trihydrate, lanthanum(III) acetylacetonate hydrate, Zr, Ti, Nb, and W alkoxides. The photostrictive effect and its dependence on dopant and fabrication method were investigated.

Experimental Procedure

PLZT (3/52/48) ceramics with 3 at% La and a Zr/Ti ratio of 52/48 was selected due to its highest photovoltaic effect [2]. PLZT (3/52/48) doped with 0.5 at% WO_3 and various concentrations of Nb_2O_5 were prepared by the conventional oxide mixing process and the sol–gel technique. Figure 1 illustrates a flow chart for the sample preparation by the conventional oxide mixing process. In this method, $PbCO_3$, La_2O_3, ZrO_2, TiO_2 and dopants (WO_3 or Nb_2O_5) were mixed in the proper ratio corresponding to the composition and ball milled for 48 h. The slurry was dried and calcined at 950°C for 10 h. The calcined
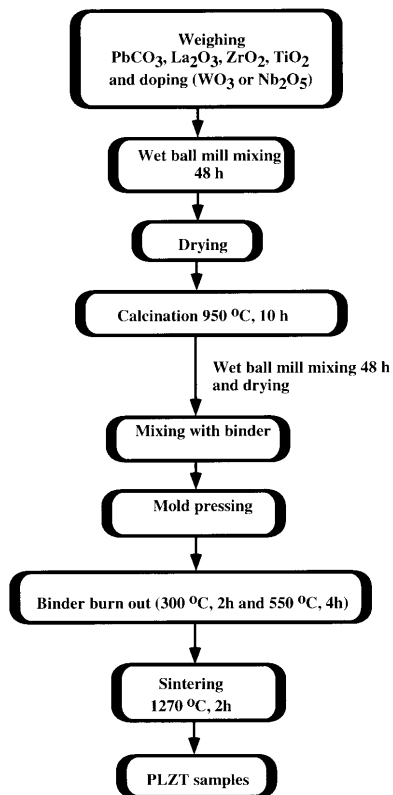
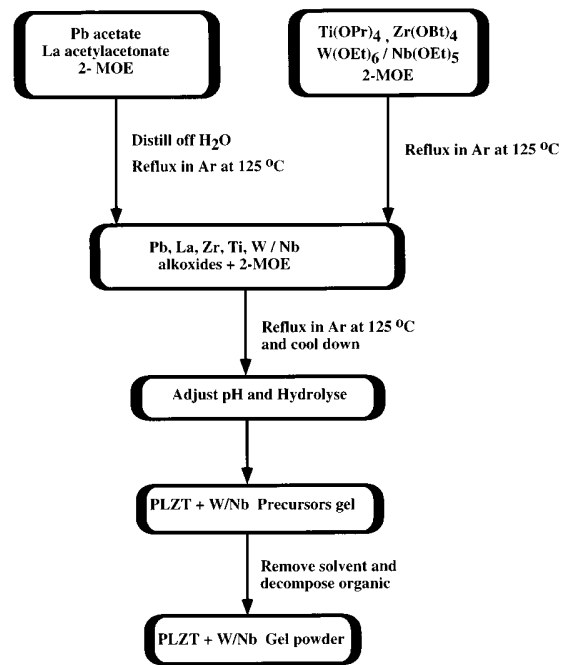*Fig. 2*. Flow diagram of sample preparation by sol–gel process. 2-MOE: 2-methoxyethanol, $Ti(OPr)_4$: Titanium(IV) isopropoxide, $Zr(OBt)_4$: Zirconium(IV) butoxide, $W(OEt)_6$: Tungsten(VI) ethoxide, $Nb(OEt)_5$: Niobium(V) ethoxide.

powder was further ball milled for 48 h and subsequently sintered in air at 1270°C for 2 h. The flow chart for the sample preparation by the sol–gel technique has been shown in Fig. 2. In the sol–gel processing, lead(II) acetate trihydrate, $Pb(CH_3COO)_2 \cdot 3H_2O$, lanthanum(III) acetylacetonate hydrate, $La(acac)_3 \cdot H_2O$, zirconium(IV) butoxide, $Zr(OC_4H_9)_4$, and titanium(IV) isopropoxide, $Ti(OC_3H_7)_4$, were used as precursors while tungsten(VI) ethoxide, $W(OC_2H_5)_6$ and niobium(V) ethoxide, $Nb(OC_2H_5)_5$, were used as dopants and 2-methoxyethanol (2-MOE) was used as a solvent. Pb and La precursors were mixed in the proper ratio and dissolved in 2-MOE and used as precursor site A. The solution was distilled and refluxed at 125°C and cooled to room temperature. Precursor site B comprising of Zr, Ti and dopant were mixed in the proper ratio using 2-MOE as a solvent. The solution was refluxed in Ar at 125°C and cooled to room temperature. Subsequently, the solution was added into the reflux solution of site A and was refluxed in Ar at 125°C. The pH of this solution was adjusted to 10 by using nitric acid, before its hydrolysis. The solution was then aged to yield a gel which was dried

Fig. 1. Flow diagram of sample preparation by oxide mixing process.

to obtain the powder. After the removal of organics at 400°C for 6 h, the powder was calcined at 600°C for 1 h and sintered at 1250°C for 2 h in air.

The density of the sintered samples was determined by the Archimedes method. Microstructure and grain size of the samples were observed by scanning electron microscopy (ISI-SX-40X Scanning Electron Microscope, International Scientific Instruments, Inc., NY). Dielectric properties of PLZT samples were measured with an impedance analyzer (HP-4274A). Samples for dielectric measurements were polished to about 10 mm in diameter and 1 mm in thickness, then electroded with platinum (Pt) by sputtering. Piezoelectric properties of all the samples were measured by using a Berlincourt d_{33} meter (Channel Products, Inc.) at 100 Hz. Samples for piezoelctric measurement were of the same configuration as for dielectric measurements, except they were poled in silicone oil at 120°C under a 2 kV/mm electric field for 10 min.

Photovoltaic measurements were done by using a high-input-impedance electrometer (Keithley 617), while the photostriction measurement was done by using the displacement sensor (LVDT, Millitron model 1301). These measurements were done by radiating the light perpendicular to the polarization direction. The samples of $5 \times 5 \times 1 \, mm^3$ were cut and polished for these measurements. The $5 \times 1 \, mm^2$ surfaces were silver electroded. Poling was performed by applying 2 kV/mm electric field for 10 min. in silicone oil at 120°C. A high pressure mercury lamp (Ushio Electric USH-500D) was used as a light source for the measurement. The white radiation was passed through an IR blocking filter and an UV bandpass filter to obtain a beam with a maximum strength
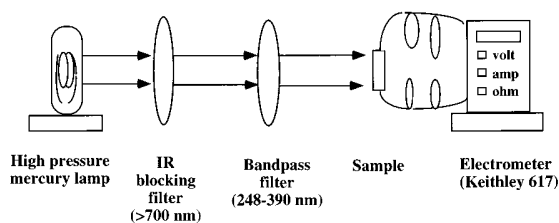

Fig. 3. Experimental set up for photovoltaic measurement.
Illumination
 – High pressure mercury lamp
 – Without polarizer
 – Filter   – IR blocking filter
                   – Bandpass filter
 – Wavelength – 370 nm
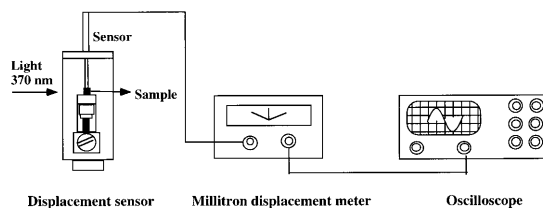 – Intensity   – 3.25 mW/cm².

Fig. 4. Experimental set up for photostrictive measurement.

around 370 nm and an intensity of $3.25 \, mW/cm^2$, before illuminating the samples ($5 \times 5 \, mm^2$ polished surface). The light beam with this wavelength has been reported to yield the maximum photovoltaic properties (Uchino et al., 1985). The experimental set-up for photovoltaic and photostriction measurements are shown in Figs. 3 and 4, respectively.

Results and Discussion

Relative Density

Figure 5 shows the relative sintered density of Nb_2O_5 doped PLZT as a function of sintering temperature. A relative density of 98% was achieved for PLZT oxide samples sintered at 1200°C. The sintered density saturated and remained constant as the sintering temperature increased to 1300°C. On the other hand, in the sol–gel PLZT a maximum density of 91% was observed at a sintering temperature of 1250°C. The
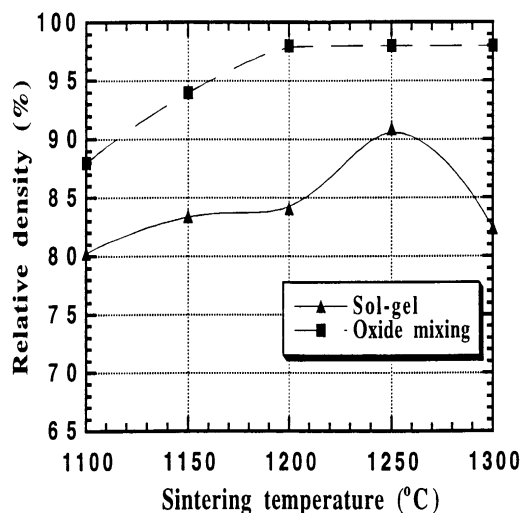

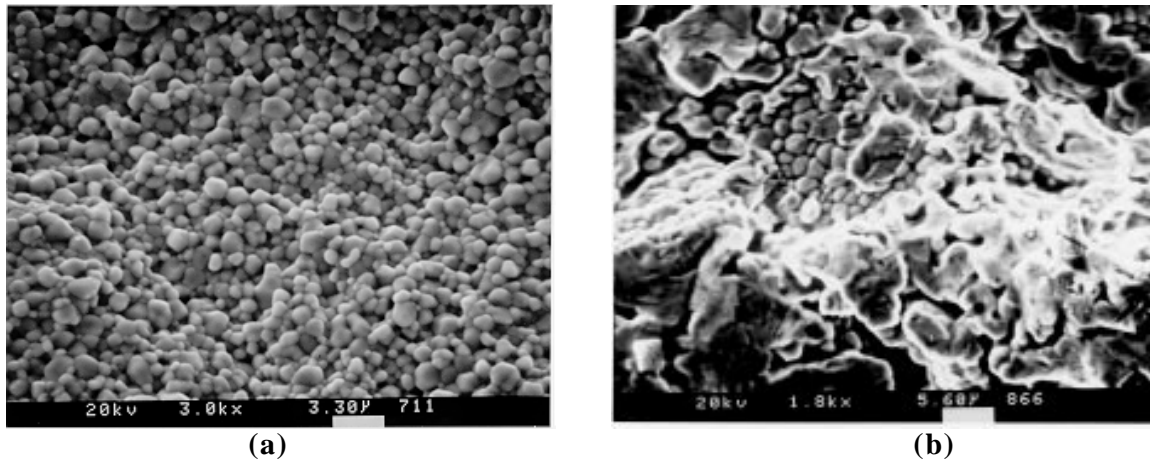Fig. 5. Relative density as a function of sintering temperature after 2 h sintering.

Fig. 6. SEM micrographs of 1.0 at% Nb$_2$O$_5$ doped PLZT ceramics prepared by (a) oxide mixing (b) sol–gel methods.

sintered density decreased as the sintering temperature was further increased. This was probably due to the evaporation of PbO during sintering. As evident from Fig. 5, the sol–gel PLZT exhibits lower density as compared to the oxide PLZT at all the sintering temperatures. This lower density was probably due to finer and agglomerated particles, resulting in aggregation which was observed in some areas of Nb$_2$O$_5$ doped sol–gel PLZT. However, the aggregation was not observed in 0.5 at% WO$_3$ doped sol–gel PLZT, which is one reason for the higher relative density of this ceramic (93%) than Nb$_2$O$_5$ doped sol–gel PLZT. The high density in PLZT oxide samples is probably

due to higher packing density without agglomeration as compared to sol–gel ceramics. Figure 6 shows the SEM micrographs of the sintered ceramic surfaces. The 1.0 at% Nb$_2$O$_5$ doped sol–gel PLZT in (b) clearly showed large pores which were caused by the particle agglomeration.

Grain Size

The average grain size is shown in Fig. 7 as a function of doping concentration. The average grain size decreases with increasing doping concentration. Nb$_2$O$_5$ was found to be more effective in suppressing
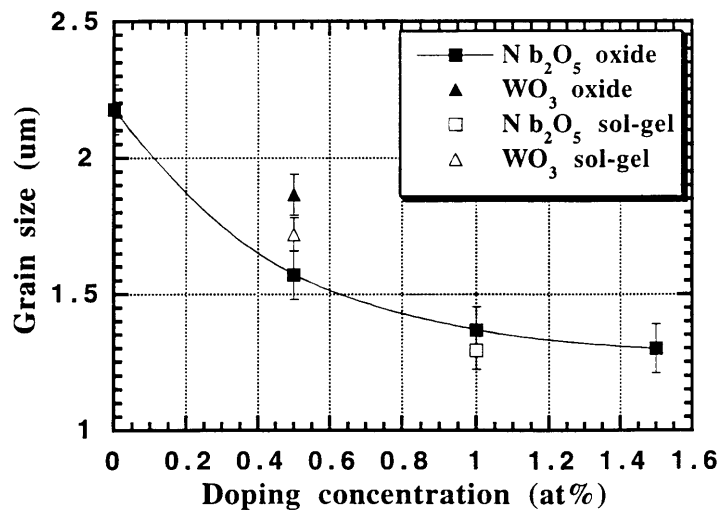

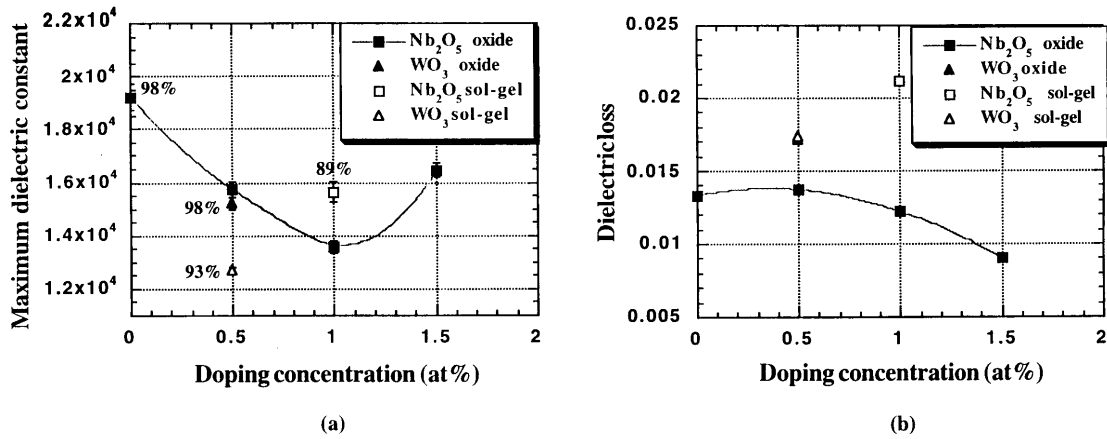*Fig. 7.* Variation of average grain size with doping concentration.

Fig. 8. Variation of (a) maximum dielectric constant (b) maximum dielectric loss with doping concentration.

the grain size as compared to WO_3 as a dopant. The grain size of the sol–gel ceramics was smaller than that of the oxide mixing ceramics when sintered at 1250°C for 2 h.

Dielectric and Piezoelectric Properties

Figure 8(a) shows the change in the maximum dielectric constant with doping concentration. The number shown in the figure represents the relative density of the samples at each composition. The dielectric loss $(\tan \delta)$ as a function of doping concentration is shown in Fig. 8(b). The maximum dielectric constant was found to decrease with increasing doping concentration for the case of oxide mixing samples. This was partially due to the lower grain size observed in PLZT doped oxide mixing ceramics. The dielectric constant showed a minimum at 1.0 at% Nb_2O_5 doped oxide PLZT. Also, the sol–gel PLZT doped with WO_3 has a lower dielectric constant compared to the oxide PLZT due to the smaller grain size. However, the Nb_2O_5 doped sol–gel PLZT exhibits higher dielectric constant as compared to the oxide PLZT at the same composition.
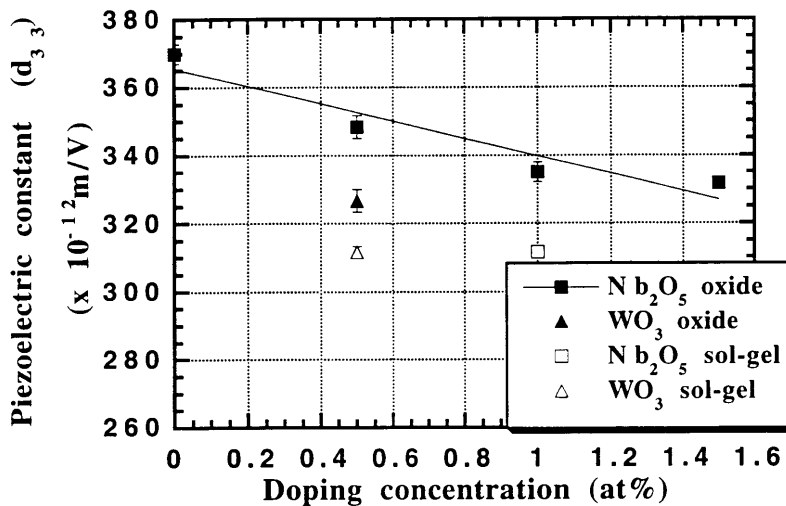

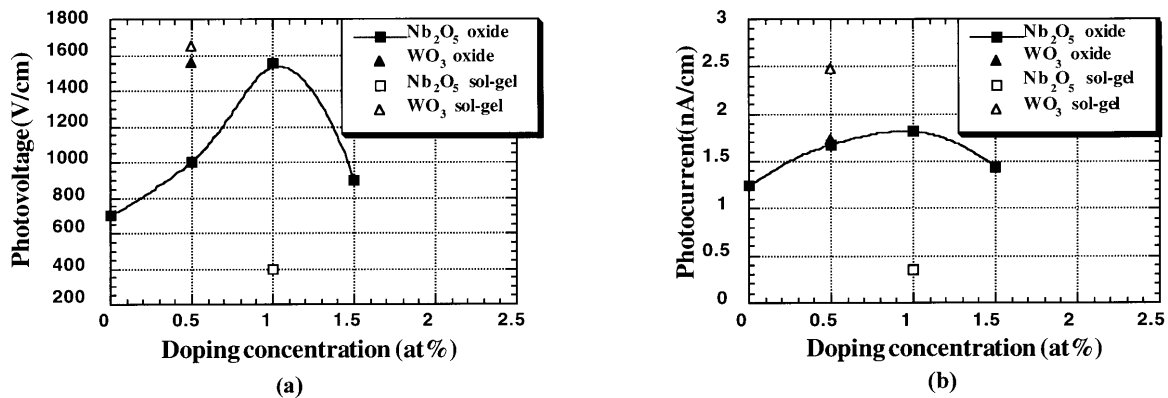Fig. 9. Variation of piezoelectric constant with doping concentration.

Fig. 10. Variation of (a) photovoltage (b) photocurrent with doping concentration.

This may be due to the high dielectric loss observed in this ceramic (Fig. 8(b)). Higher dielectric loss in sol–gel samples may be due to loss through grain boundaries and pores.

The piezoelectric constant as a function of doping concentration is shown in Fig. 9. The measured value of d_{33} decreases with increasing doping concentration. Also, the sol–gel ceramics exhibit lower d_{33} as compared to the oxide ceramics. With decrease in grain size, the domain wall contribution to the piezoelectric properties drops off, leading to this decrease in piezoelectric constant.

Photovoltaic and Photostrictive Properties

Figure 10 shows the variation of photovoltaic responses with doping concentration for the samples doped with WO_3 and Nb_2O_5. All dopants were found to enhance the photovoltaic responses. The photo-voltage reached more than $1\,kV/cm$ and the photocurrent was of the order of nA/cm. As in the previous papers, the current density was normalized only with respect to the width of the illuminated surface, but not to the depth. Both the photovoltage and photocurrent revealed a maximum at 1 at% of doped Nb_2O_5 in the oxide PLZT. WO_3 doped sol–gel PLZT showed the maximum photovoltaic response among all the samples. This may be attributed to higher degree of homogeneity and uniform distribution of dopant and a stoichiometry in compositions for this sample. Lower photovoltaic properties were observed in Nb_2O_5 doped sol–gel PLZT. In general, increase in photovoltage will enhance photostriction and increasing photocurrent will increase the response speed. The photostriction is estimated as the product of the photovoltage and the piezoelectric coefficient (Uchino and Aizawa, 1985, Sada et al., 1987; Chu and Uchino, 1995). It can be expressed by
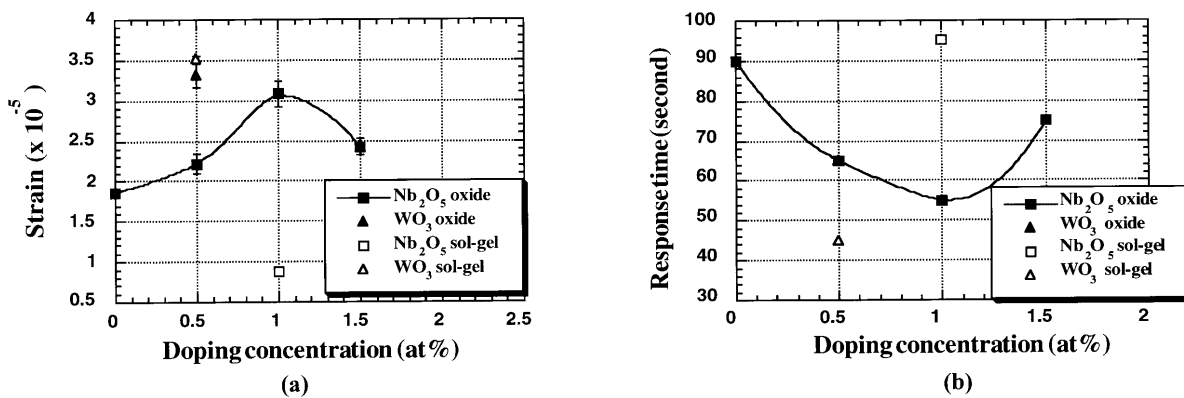

Fig. 11. Variation of (a) photoinduced strain (b) response time with doping concentration.

$$x_{ph} = d_{33}E_{ph}(1 - \exp(-t/RC))$$

where x_{ph} is photoinduced strain, d_{33} is piezoelectric coefficient, E_{ph} is the saturated photovoltage, t is time, R is the resistance, and C is the capacitance of samples. RC is referred to as time constant or response speed which suggests that a sample with high photocurrent will give fast response speed as compared to slow response samples. These effects are confirmed in Figs. 11(a) and 11(b), where the change in photostriction and response speed are shown as a function of doping concentration. Similar changes in photovoltaic behavior with doping concentration was observed in the photostrictive effect. The maximum photostriction was found in WO_3 doped sol–gel PLZT. In the Nb_2O_5 doped oxide PLZT, the largest photostriction was observed in the sample with 1.0 at% Nb_2O_5. Also, the WO_3 doped sol–gel PLZT exhibited the fastest response time among all the samples. The fastest response time among Nb_2O_5 doped oxide PLZT, was obtained at 1.0 at% Nb_2O_5. The lower photostriction and the slow response speed in Nb_2O_5 doped sol–gel PLZT can be due to the agglomeration of fine powder which resulted in a lower density.

Conclusions

WO_3 and Nb_2O_5 were effective in suppressing the grain growth which leads to the enhancement of photovoltaic and photostrictive properties in PLZT. Although WO_3 was less effective in suppressing the grain size, due to its inherent dopant property, it was more effective in enhancing the photovoltaic and photostrictive responses. Dielectric and piezoelectric properties were found to decrease with increasing doping concentration due to the smaller grain size. In general, the dielectric and piezoelectric properties can be enhanced by doping with donors such as WO_3 and Nb_2O_5. However, they also decrease with decreasing grain size due to a drop in domain wall contribution. The lower dielectric and piezoelectric properties found in doped ceramics indicate the dominance of the grain size effect. Although the relative density of sol–gel PLZT is lower than oxide PLZT at the same composition, the preliminary results showed that the maximum photovoltaic and photostrictive effect were obtained for 0.5 at% WO_3 doped sol–gel PLZT. This may suggest that a better homogeneity and a closer control of stoichiometry in sol–gel technique as compared to oxide mixing process give rise to higher photovoltaic and photostrictive properties. The aggregation and low density observed in Nb_2O_5 doped sol–gel PLZT was the reason for lower photovoltaic and photostrictive responses as compared to the WO_3 doped sol–gel PLZT.

In conclusion, the preliminary results in this study suggest that the sol–gel technique possesses the possibility in enhancing the photostriction in PLZT. It must also be noted that if the density of sol–gel processed PLZT can be increased through particle size distribution and by controlling the agglomeration, even further improvement in photostrictive response will be achieved.

Bibliography

Chiou, B.-S. and Kno, J.N., 1990, The Preparation of PLZT Ceramics from a Sol-Gel Process, *J. Elec. Mater.*, **19**(4), 393–397.

Chu, S.-Y. and Uchino, K., 1995, Photostrictive Effect in PLZT-Based Ceramics and its Application, *Ferroelectrics*, **174**, 185–196.

Chu, S.-Y., Ye, Z., and Uchino, K., 1994, Photovoltaic Effect for the Linearly Polarized Light in (Pb, La) (Zr, Ti) O_3 Ceramics, *Smart Mater. Struct.*, **3**, 114–117.

Rahaman, M.N., 1995, Ceramic Processing and Sintering, Marcel Dekker Inc., New York, 207.

Sada, T., Inoue, M., and Uchino, K., 1987, Photostriction in PLZT Ceramics, *J. Ceram. Soc. Jpn.*, Inter. Ed., **95**, 499–504.

Uchino, K. and Aizawa, M., 1985, Photostrictive Actuator Using PLZT Ceramics, *Jpn. J. Appl. Phys. Suppl.*, **24**, 139–141.

Uchino, K., Aizawa, M., and Nomura, S., 1985, Photostrictive Effect in (Pb, La) (Zr, Ti) O_3, *Ferroelectrics*, **64**, 199–208.

Xu, Y., 1991, Ferroelectric Materials and Their Application, Elsevier Science Pub. Co., New York, 164.